

Structural and Functional Studies of *Aspergillus oryzae* Cutinase: Enhanced Thermostability and Hydrolytic Activity of Synthetic Ester and Polyester Degradation

Zhiqiang Liu,[†] Yuying Gosser,[‡] Peter James Baker,[†] Yaniv Ravee,[†] Ziyang Lu,[‡]
Girum Alemu,[‡] Huiguang Li,[§] Glenn L. Butterfoss,^{||} Xiang-Peng Kong,[§]
Richard Gross,[†] and Jin Kim Montclare^{*,†,⊥}

Department of Chemical and Biological Sciences, Polytechnic Institute of New York University, Brooklyn, New York 11201, Pathways Bioinformatics & Biomolecular Center, The City College, CUNY, New York, New York 10031, Department of Biochemistry, NYU School of Medicine, 550 First Avenue, New York, New York 10016, Department of Biology and Computer Science, New York University, New York, New York 10003, Department of Biochemistry, SUNY-Downstate Medical Center, Brooklyn, New York 11203

Received June 8, 2009; E-mail: jmontcla@poly.edu

Abstract: Cutinases are responsible for hydrolysis of the protective cutin lipid polyester matrix in plants and thus have been exploited for hydrolysis of small molecule esters and polyesters. Here we explore the reactivity, stability, and structure of *Aspergillus oryzae* cutinase and compare it to the well-studied enzyme from *Fusarium solani*. Two critical differences are highlighted in the crystallographic analysis of the *A. oryzae* structure: (i) an additional disulfide bond and (ii) a topologically favored catalytic triad with a continuous and deep groove. These structural features of *A. oryzae* cutinase are proposed to result in an improved hydrolytic activity and altered substrate specificity profile, enhanced thermostability, and remarkable reactivity toward the degradation of the synthetic polyester polycaprolactone. The results presented here provide insight into engineering new cutinase-inspired biocatalysts with tailor-made properties.

Introduction

With environmental concerns over waste build-up and limited petroleum resources, the demand has never been greater for enzymatic or “green” approaches for efficient chemical synthesis and degradation reactions.^{1–3} Several enzymes have been exploited not only to perform stereo- and regioselective chemical transformations on small molecules but also to break down or modify synthetic polymers useful for applications in chemical, pharmaceutical, and textile industries.^{2,4,5} Serine hydrolases have been employed most extensively for these biotransformations.^{1,6–14}

Cutinases are α/β hydrolases commonly secreted by fungal phytopathogens that enable them to penetrate the protective surface cutin layer of plants.^{15–19} Cutin is an insoluble, cross-linked, lipid-polyester matrix comprised of *n*-C₁₇ and *n*-C₁₈ hydroxy and epoxy fatty acids that serve as a barrier against dehydration and invasion. Cutinases hydrolyze and break down these complex polyesters into smaller hydroxyacids.^{15,19}

Because of the ability of cutinases to hydrolyze cutin, they have been exploited for reactions with small molecule esters and synthetic polyesters.¹ The utility of cutinase or any enzyme

[†] Polytechnic Institute of New York University.

[‡] The City College, CUNY.

[§] NYU School of Medicine.

^{||} New York University.

[⊥] SUNY-Downstate Medical Center.

- (1) Carvalho, C. M. L.; Aires-Barros, M. R.; Cabral, J. M. S. *Biotechnol. Bioeng.* **1999**, *66*, 17–34.
- (2) Guebitz, G. M.; Cavaco-Paulo, A. *Trends Biotechnol.* **2008**, *26*, 32–38.
- (3) Maeda, H.; Yamagata, Y.; Abe, K.; Hasegawa, F.; Machida, M.; Ishioka, R.; Gomi, K.; Nakajima, T. *Appl. Microbiol. Biotechnol.* **2005**, *67*, 778–788.
- (4) Costa, L.; Brissos, V.; Lemos, F.; Ribeiro, F. R.; Cabral, J. M. S. *Bioprocess Biosyst. Eng.* **2008**, *31*, 323–327.
- (5) Liu, Y. B.; Wu, G. F.; Gu, L. H. *AATCC Rev.* **2008**, *8*, 44–48.
- (6) Masaki, K.; Kamini, N. R.; Ikeda, H.; Iefuji, H. *Appl. Environ. Microbiol.* **2005**, *71*, 7548–7550.
- (7) Vidinha, P.; Harper, N.; Micaelo, N. M.; Lourenço, N. M. T.; da Silva, M.; Cabral, J. M. S.; Afonso, C. A. M.; Soares, C. M.; Barreiros, S. *Biotechnol. Bioeng.* **2004**, *85*, 442–449.

- (8) Borreguero, I.; Carvalho, C. M. L.; Cabral, J. M. S.; Sinisterra, J. V.; Alcantara, A. R. *J. Mol. Catal. B: Enzym.* **2001**, *11*, 613–622.
- (9) Bogel-Lukasik, R.; Lourenço, N. M. T.; Vidinha, P.; da Silva, M.; Afonso, C. A. M.; da Ponte, M. N.; Barreiros, S. *Green Chem.* **2008**, *10*, 243–248.
- (10) Chen, B.; Hu, J.; Miller, E. M.; Xie, W. C.; Cai, M. M.; Gross, R. A. *Biomacromolecules* **2008**, *9*, 463–471.
- (11) Kulshrestha, A. S.; Gao, W.; Fu, H. Y.; Gross, R. A. *Biomacromolecules* **2007**, *8*, 1794–1801.
- (12) Chen, B.; Miller, E. M.; Miller, L.; Maikner, J. J.; Gross, R. A. *Langmuir* **2007**, *23*, 1381–1387.
- (13) Azim, H.; Dekhterman, A.; Jiang, Z. Z.; Gross, R. A. *Biomacromolecules* **2006**, *7*, 3093–3097.
- (14) Hu, J.; Gao, W.; Kulshrestha, A.; Gross, R. A. *Macromolecules* **2006**, *39*, 6789–6792.
- (15) Purdy, R. E.; Kolattukudy, P. E. *Biochemistry* **1975**, *14*, 2824–2831.
- (16) Longhi, S.; Czjzek, M.; Lamzin, V.; Nicolas, A.; Cambillau, C. *J. Mol. Biol.* **1997**, *268*, 779–799.
- (17) Sweigard, J. A.; Chumley, F. G.; Valent, B. *Mol. Gen. Genet.* **1992**, *232*, 174–182.
- (18) Martínez, C.; Degeus, P.; Lauwereys, M.; Matthysens, G.; Cambillau, C. *Nature* **1992**, *356*, 615–618.
- (19) Purdy, R. E.; Kolattukudy, P. E. *Biochemistry* **1975**, *14*, 2832–2840.

for chemical reactions is commonly limited by intolerance to high temperatures and the constraints of the substrate recognition pocket.¹ Thus, the identification of enzymes exhibiting enhanced thermostability and altered reactivity for various substrates would greatly expand the potential of cutinase for industrial and environmental applications.

Aspergillus oryzae is a filamentous fungus that has been employed in fermentation to produce traditional consumable products such as rice wine, soybean paste, and soy sauce in the food industry for approximately 1000 years.⁹ It has been used recently as an expression host for recombinant proteins²⁰ and to degrade poly(butylene succinate) (PBS) as well as emulsified poly(butylenes succinate-*co*-adipate) (PBSA).³ Because of the remarkable ability of *A. oryzae* cutinase to readily break down such synthetic plastics,³ it represents an excellent target to perform detailed structure–activity analysis. Here we report the reactivity, stability, and crystal structure of *A. oryzae* cutinase and perform a comparison to the well-characterized *Fusarium solani* cutinase.

Methods

Enzyme Expression. The cutinase gene was expressed in *Pichia pastoris*, and recombinant cutinase was produced by using the strong methanol-induced AOX1 promoter. Single colonies were picked and cultured in BMGY medium (g/L) composed of 5 g of yeast extract, 10 g of peptone, supplemented with 50 mL of 1 M KH₂PO₄ buffer pH 6.0, 1.7 g of yeast nitrogen base, 5 g of ammonium sulfate, 5 mL of glycerol, 500 × 1 mL biotin, and 96 × 5.2 mL histidine. Precultures of *P. pastoris* harboring cutinase genes were incubated at 30 °C, 200 rpm, overnight. After centrifugation at 6,000 rpm for 10 min, cells were transferred into a parallel fermentor (DASGIP, Germany) containing 1 L of basal salt medium composed of glycerol 40 mL/L, CaSO₄ 0.9 g/L, K₂SO₄ 14.67 g/L, MgSO₄·7H₂O 11.67 g/L, (NH₄)₂SO₄ 9 g/L, 12 mL/L hexameta-phosphate, trace salts (cupric sulfate·5H₂O 6.0 g/L, sodium iodide 0.08 g/L, manganese sulfate H₂O 3.0 g/L, sodium molybdate·2H₂O 0.2 g/L, boric acid 0.02 g/L, cobalt chloride 0.5 g/L, zinc chloride 20.0 g/L, ferrous sulfate·7H₂O 65 g/L, biotin 0.2 g/L). The constant dissolved oxygen was set to 40%, glycerol (50%, v/v) feeding time was 6 h, and the rate of methanol feeding was 5 mL/h. When the activity reached its maximum, the fermentation was stopped. After centrifugation, the supernatant was collected for further use.

Enzyme Purification. Fermentation broth was centrifuged at 8,000 rpm for 10 min at 4 °C, and then supernatant was concentrated about 10 times using an ultrafiltration unit (Millipore TFE system) with a 10 kDa membrane. Cutinase was purified by FPLC using VISION Workstation (Applied Biosystems Co.) with a 16 mmD/100 mmL POROS MC 20 μm column (Applied Biosystems Co.). The metal site in the column was saturated with NiCl₂ solution according to operating instructions for the column. Approximately 50 mM NaH₂PO₄ buffer with 0.5 mM imidazole (pH 8.0) was used as a starting buffer, and 50 mM NaH₂PO₄ buffer with 100 mM imidazole (pH 8.0) was used as an elution buffer at a flow rate of 30 mL/min. Samples filtered by a 0.45 μm filter were loaded onto the column. Approximately 2 column volumes (CVs) of starting buffer were run to wash out any proteins that were bound nonspecifically to the column, and then 3 CVs of elution buffer with imidazole were run with a concentration linear gradient from 0 to 100 mM. The peak fraction in the gradient step was collected. The collected samples were desalted by an ultrafiltration unit with a 10 kDa membrane and then freeze-dried. SDS–PAGE analysis of the purified proteins was performed (Supporting Information).

Kinetic Analysis for pNP Ester Substrates. The pNP esters (pNPA, pNPB, pNPV, and pNPH) with concentration ranging from

60 to 0.9375 μM were used for the kinetic study.^{21,22} Assays were performed using a final concentration of 1.1 μM of *A. oryzae* and *F. solani* cutinases in 14.5 mM Tris-HCl buffer pH 7.5, 0.75% glycerol. Since pNPA and pNPH were dissolved in DMSO, pNPB in methanol, and pNPV in TritonX, there was approximately 25% DMSO, methanol or 0.5% Triton X in the final mixtures.²³ Reactions were initiated by the addition of enzyme, and reaction progress was monitored spectrophotometrically (Molecular Devices Spectramax M2) at 405 nm. Softmax Pro v5 software was used to analyze data. Enzyme-catalyzed initial rates were corrected by subtracting background hydrolysis rate. All reactions were performed in triplicate. The K_m and k_{cat} values were determined by a double-reciprocal Lineweaver–Burk plot (1/ v vs 1/[pNPA/pNPB/pNPV/pNPH]) (Supporting Information).

Thermoactivity. The thermoactivity or residual activity of cutinases was investigated by incubating enzymes at temperatures ranging from 25 to 60 °C at a final concentration of 1.1 μM in 14.5 mM Tris-HCl buffer pH 7.5, 0.75% glycerol. The incubation took place in an Eppendorf Thermomixer at the specified temperature with a constant mixing of 350 rpm for 1 h. The samples were incubated on ice for 5 min followed by incubation at room temperature for 15 min. Reactions were initiated by addition of 30 μM pNPB, monitored at 405 nm for 1 min, and performed in triplicate. The data obtained was presented as activity without normalization.

Circular Dichroism (CD) Measurements. CD spectra were recorded on a JASCO J-815 Spectropolarimeter using Spectra Manager 228 software. Temperature was controlled using a Fisher Isotemp Model 3016S water bath. A protein concentration of 29 μM in 10 mM sodium phosphate buffer, pH 8.0 was used for both cutinases. Data were collected at 1-nm intervals from 190 to 250 nm for wavelength scans and 0.3 °C/min from 4 to 85 °C for temperature scans in duplicate (Supporting Information). Small signaling arising from buffer was subtracted.

Thermodynamic Parameters by Differential Scanning Calorimetry (DSC). Calorimetric measurements of melting temperatures (T_m) were carried out on a NanoDSC differential scanning calorimeter (TA Instruments) with a sample cell volume of 0.3 mL. Unfolding data of both cutinases were obtained by heating the samples, at a concentration 5 mg/mL, from 4 to 80 °C at a rate of 1 °C/min in duplicate (Supporting Information). The protein samples were present in water. Water was used in the reference cell to obtain the molar heat capacity by comparison. The observed thermograms were baseline corrected, and normalized data were analyzed using NanoAnalyze software.

Degradation of Polymer Thin Films. Thin films of poly(ϵ -caprolactone) (PCL) were cut to 1.0 cm × 1.0 cm with an approximate thickness of 250 μm (30–35 mg) and placed in 20 mL scintillation screw cap vials containing 2.5 mL of 100 mM Tris-HCl buffer pH 8.0 with a final concentration of 8.8 μM enzyme. The control vials contained a film with buffer solution. All measurements were performed in triplicate, incubated for 6 h at 40 °C in an incubator shaker at 200 rpm, and weighed after drying.

Crystallization. The protein was crystallized by mixing equal volumes of protein solution (15 mg/mL, in 100 mM Tris buffer pH 8.5) with mother liquor (30% PEG2KME, 100 mM potassium thiocyanate) at 296 K. The screening was conducted with 96 crystallization conditions at 296 K using the hanging drop vapor diffusion technique. Crystals appeared within 10–15 days.

Structure Determination. X-ray diffraction data of the crystal were collected at beamline X4A ($\lambda = 0.96785$ Å) of the synchrotron light source in the Brookhaven National Laboratory. Prior to data

(20) Christensen, T.; Woeldike, H.; Boel, E.; Mortensen, S. B.; Hjortshoejk, K.; Thim, L.; Hansen, M. T. *Biotechnology* **1988**, *6*, 1419–1422.

(21) Pedersen, S.; Nesgaard, L.; Baptista, R. P.; Melo, E. P.; Kristensen, S. R.; Otzen, D. E. *Biopolymers* **2006**, *83*, 619–629.
 (22) Goncalves, A. M.; Serro, A. P.; Aires-Barros, M. R.; Cabral, J. M. S. *Biochim. Biophys. Acta* **2000**, *1480*, 92–106.
 (23) Camacho, R. M.; Mateo, J. C.; González-Reynoso, O.; Prado, L. A.; Córdova, J. J. *Ind. Microbiol. Biotechnol.* **2009**, *36*, 901–909.

collection, the crystal was soaked for 5 min in a mixture of the mother liquid (30% PEG2000MME and 100 mM potassium thiocyanate) and 15% glycerol for cryoprotection. A data set of 1.75 Å resolution was collected from a single crystal at 100 K with 98.5% completeness. This data set was processed using HKL2000 software.²⁴ The crystal belongs to the trigonal space group $P3_221$ with one subunit in the asymmetric unit. The unit cell parameters were $a = 45.299$ Å, $b = 45.299$ Å, $c = 157.111$ Å and $\alpha = 90.00^\circ$, $\beta = 90.00^\circ$, $\gamma = 120.00^\circ$. The structure was solved by molecular replacement using the Molrep program in the CCP4 suite.²⁵ The structure of the native *F. solani* cutinase (PDB accession number 1CEX) was used as the search model. The initial model was built using O program. The structure was refined with CNS.²⁶ The iterative model building and refinement was carried out to a final R-work factor of 19.4% and a final free-R factor of 19.9%. The stereochemistry of the final structure was verified using the Procheck_NT and Sfccheck programs in the CCP4 suite.²⁵ Procheck validation of local geometry revealed that 91.5% of residues are located in the most favored regions of the Ramachandran plot, 7.2% are in the additional allowed regions, and 1.3% are in the generously allowed region. The electron densities of the first 10 N-terminal residues (17–25) were not observed. Structural analysis was performed using UCSF Chimera software (<http://www.cgl.ucsf.edu/chimera>).²⁷ Electrostatic surface rendering was performed using ICN and the groove by the active site was generated by the PocketFinder function.²⁸ For all above analysis 1CEX pdb file was used for *F. solani* cutinase.

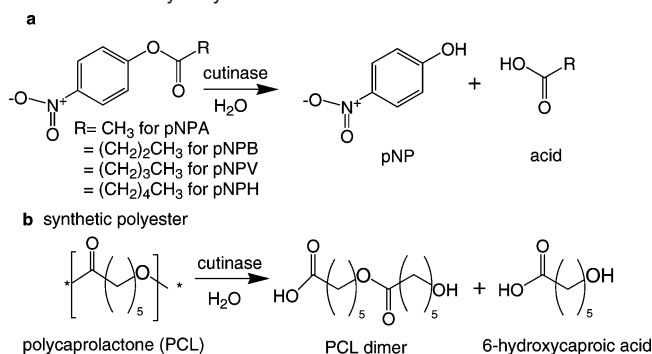
Modeling. 1CEX and the *A. oryzae* cutinase crystal structure presented here were modeled with the butyrate, valerate, and hexanoate esters of the active site serine. Hydrogens were added, and starting structures of the serine esters were generated by sampling all combinations of -60° , 60° , and 180° for each χ angle (with the exception of the ester C–O torsion, which was sampled at -180° and 180°). This generated 162, 486, and 1458 conformations for the butyrate, valerate, and hexanoate esters, respectively. The modified serine residues were then subject to 11×20 steps of conjugate gradient energy minimization using the CHARMM22 potential²⁹ while keeping all other protein atoms fixed. Modeling was done using the SIGMA package.³⁰

Results

Altered Specificity of *A. oryzae* Cutinase for pNP Esters.

Initially, the *A. oryzae* and *F. solani* cutinases were assessed for hydrolytic activity on a set of model *p*-nitrophenylester substrates: *p*-nitrophenylacetate (pNPA), *p*-nitrophenylbutyrate (pNPB), *p*-nitrophenylvalerate (pNPV), and *p*-nitrophenylhexanoate (pNPH) (Scheme 1a).^{3,10} The influence of chain length

Scheme 1. (a) Synthetic Ester and (b) Polyester Used As Substrates for Hydrolytic Reactions with Cutinase^a



^a Abbreviations: *p*-nitrophenylacetate, pNPA; *p*-nitrophenylbutyrate, pNPB; *p*-nitrophenylvalerate, pNPV; *p*-nitrophenylhexanoate, pNPH; polycaprolactone, PCL.

on cutinase activity was studied via Michaelis–Menten kinetics. The *A. oryzae* cutinase demonstrated a preference for pNPV resulting in a K_m of 0.04 ± 0.01 μM , followed by pNPB and pNPH with K_m 's of 0.21 ± 0.04 and 0.29 ± 0.09 μM , respectively. The short pNPA chain yielded a >120-fold higher K_m of 4.96 ± 0.11 μM (Table 1). The highest catalytic efficiency was observed for pNPB and pNPV with a k_{cat}/K_m of 3.49 ± 0.51 and 3.32 ± 0.74 $\mu\text{M}^{-1} \text{min}^{-1}$ (Table 1). This was followed by pNPH and pNPA with a k_{cat}/K_m of 1.34 ± 0.48 and 0.07 ± 0.01 $\mu\text{M}^{-1} \text{min}^{-1}$, respectively. This is in stark contrast to *F. solani* cutinase, where an overall preference for short chain substrate pNPA was highest. Although recognition for all three substrates was relatively similar with K_m 's ranging from 0.67 ± 0.23 to 1.50 ± 0.19 μM , the catalytic efficiencies reveal a strong preference for pNPA with a k_{cat}/K_m of 2.53 ± 1.11 $\mu\text{M}^{-1} \text{min}^{-1}$ followed by pNPV, pNPB, and pNPH, respectively (Table 1). For pNPV, pNPB and pNPH, a 6-, 10-, and 20-fold decrease in k_{cat}/K_m was observed relative to pNPA.

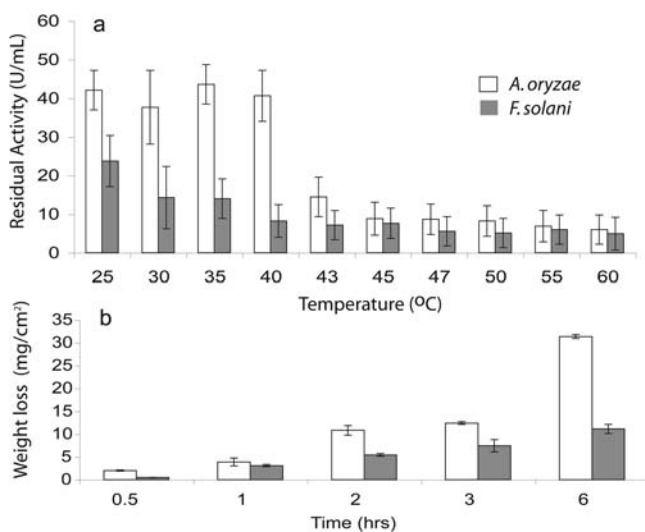
Higher Thermostability of *A. oryzae* Cutinase. To investigate the ability of the two enzymes to function at higher temperatures, we examined the residual activities for pNPB hydrolysis for a range of temperatures. Selection of pNPB was based on the demonstration of reasonable reactivity by both cutinases. The *A. oryzae* cutinase exhibited a higher activity for pNPB relative to that of *F. solani* at room temperature, corresponding to previous kinetic measurements. The level of activity was maintained even up to 40 °C in the case of *A. oryzae* cutinase (Figure 1a). By contrast, *F. solani* enzyme revealed a 40% drop at 30 °C and demonstrated a continuous decline in activity as a function of increasing temperature. Surprisingly, under all temperatures investigated, *A. oryzae* cutinase displayed higher overall residual activity when compared to that of *F. solani*, suggesting an improved tolerance to heat. This is corroborated by thermostability measurements by CD in which *A. oryzae* cutinase exhibited a higher melting temperature (T_m) of 59 °C, whereas the T_m of *F. solani* is 56 °C (Table 1). This increase in T_m is manifested by a 39.6 kJ/mol increase in enthalpy by *A. oryzae* cutinase as measured by DSC (Table 1).

Higher Reactivity of *A. oryzae* Cutinase for Synthetic Polyester. Since the natural function of cutinase is to degrade the complex biopolyester of cutin,¹⁵ we assessed the ability of both *A. oryzae* and *F. solani* enzymes to react on the surrogate, well-defined polyester, poly ϵ -(caprolactone) (PCL) (Scheme 1b). PCL is known to be degraded by various microorganisms including fungi.^{31,32} Murphy and co-workers demonstrated that

- (24) Otwinowski, Z.; Minor, W. *Methods Enzymol.* **1997**, *276*, 307–326.
 (25) Bailey, S. *Acta Crystallogr., Sect. D: Biol. Crystallogr.* **1994**, *50*, 760–763.
 (26) Brunger, A. T.; Adams, P. D.; Clore, G. M.; DeLano, W. L.; Gros, P.; Grosse-Kunstleve, R. W.; Jiang, J. S.; Kuszewski, J.; Nilges, M.; Pannu, N. S.; Read, R. J.; Rice, L. M.; Simonson, T.; Warren, G. L. *Acta Crystallogr., Sect. D: Biol. Crystallogr.* **1998**, *54*, 905–921.
 (27) Pettersen, E. F.; Goddard, T. D.; Huang, C. C.; Couch, G. S.; Greenblatt, D. M.; Meng, E. C.; Ferrin, T. E. *J. Comput. Chem.* **2004**, *25*, 1605–1612.
 (28) Abagyan, R.; Totrov, M.; Kuznetsov, D. *J. Comput. Chem.* **2004**, *15*, 488–506.
 (29) MacKerell, A. D.; Bashford, D.; Bellott, M.; Dunbrack, R. L.; Evansck, J. D.; Field, M. J.; Fischer, S.; Gao, J.; Guo, H.; Ha, S.; Joseph-McCarthy, D.; Kuchnir, L.; Kuczera, K.; Lau, F. T. K.; Mattos, C.; Michnick, S.; Ngo, T.; Nguyen, D. T.; Prodhom, B.; Reiher, W. E.; Roux, B.; Schlenkrich, M.; Smith, J. C.; Stote, R.; Straub, J.; Watanabe, M.; Wiorkiewicz-Kuczera, J.; Yin, D.; Karplus, M. *J. Phys. Chem. B* **1998**, *102*, 3586–3616.
 (30) Mann, G.; Yun, R. H.; Nyland, L.; Prins, J.; Board, J.; Hermans, J., *Computational methods for macromolecules: Challenges and Applications—Proceedings of the 3rd International Workshop on Algorithms for Macromolecular Modeling*; Schlick, T., Gan, H. H., Eds.; Springer Verlag: Berlin, 2002; pp 129–145.

Table 1. Kinetic and Thermodynamic Parameters

cutinase	pNPA		pNPB		pNPV		pNPH		T_m (°C)	ΔH (kJ/mol)
	K_m (μM^{-1})	k_{cat}/K_m ($\mu\text{M}^{-1} \text{min}^{-1}$)	K_m (μM^{-1})	k_{cat}/K_m ($\mu\text{M}^{-1} \text{min}^{-1}$)	K_m (μM^{-1})	k_{cat}/K_m ($\mu\text{M}^{-1} \text{min}^{-1}$)	K_m (μM^{-1})	k_{cat}/K_m ($\mu\text{M}^{-1} \text{min}^{-1}$)		
<i>F. solani</i>	0.67 ± 0.23	2.53 ± 1.11	1.26 ± 0.28	0.26 ± 0.06	1.48 ± 0.56	0.61 ± 0.40	1.50 ± 0.19	0.14 ± 0.02	56	562.21
<i>A. oryzae</i>	4.96 ± 0.1	0.07 ± 0.01	0.21 ± 0.04	3.49 ± 0.51	0.04 ± 0.01	3.32 ± 0.74	0.29 ± 0.09	1.34 ± 0.48	59	622.61

**Figure 1.** (a) Thermoactivity profile as measured in terms of residual activity for pNPB upon incubation at increasing temperatures. (b) Weight loss measurements of defined PCL films.

F. solani strains bearing cutinase were able to degrade PCL and use it as a carbon source as well as to induce the production of cutinase,³³ suggesting that the cutinase should be active for PCL hydrolysis in vitro. PCL films with dimensions of 1 cm² and 250 μm thickness were incubated at 40 °C in the presence of either *A. oryzae* or *F. solani* cutinase in 100 mM Tris-HCl at pH 8.0. Remarkably, nearly complete degradation of 87% PCL was achieved within 6 h in the presence of *A. oryzae* enzyme. Degradation of PCL films by *F. solani* cutinase proceeded more slowly, reaching 30% degradation by 6 h (Figure 1b). These data support the results on the aforementioned substrate specificity in which the *A. oryzae* cutinase preferred longer chain esters such as pNPB and pNPH, since PCL represents a longer chain polyester. Furthermore, this supports the thermoactivity data in which a dramatic loss in activity was observed for the *F. solani* enzyme at 40 °C while that of *A. oryzae* maintained a high level activity.

Crystal Structure of *A. oryzae* Cutinase and Comparison to That of *F. solani*. To understand the observed reactivity and stability differences, the *A. oryzae* cutinase structure was determined by molecular replacement method and refined to 1.75 Å resolution (PDB ID:3GBS, Supporting Information). The crystal structure revealed a monomeric protein with an α/β fold hallmarked by a central β -sheet of 5 parallel strands surrounded by 10 α -helices. As a member of the α/β hydrolases, this enzyme possesses an active site composed of the catalytic triad residues Ser126, Asp181, and His194 (Figure 2a). The catalytic site is surrounded by the two hydrophobic surfaces composed

of residues 87–93 within helix 3, and residues 186–194 that represents the loop between helices 9 and 10 as well as the first 3 residues of the latter. *A. oryzae* cutinase bears an oxyanion hole composed of Ser48 and Gln127 backbone amides that are critical in polarizing the ester bond of the substrate and stabilizing the transition state of the formed substrate oxyanion (Figure 2a).¹²

Upon overlay, the *A. oryzae* and *F. solani* structures have a similar fold with an overall rms deviation of 1.02 Å, main chain deviation of 0.87 Å, and C α deviation of 0.84 Å (Figure 3a). However, the *A. oryzae* enzyme bears several structural features that differ significantly from that of *F. solani*. Comparison of the two sequences reveal that the *A. oryzae* cutinase is shorter than that of *F. solani* as exhibited by smaller loops in the N- and C-terminal regions as well as a missing β -strand in the *A. oryzae* structure (Figures 2a and 3a). Although the *F. solani* cutinase possesses 6 β -strands and 10 α -helices, the *A. oryzae* structure bears the 5 β -strands and the same number of α -helices. The N-terminal region (residues Thr26 to Asp30), the loops in between helix 1 and strand 1 (residues Gly35 to Pro49), as well as helix 2 and strand 2 (residues Ser71 to Asp73), helix 10 (residues Ser199 to Asp203), and C-terminal residues beyond helix 10 based on the *A. oryzae* structure deviate significantly in the overlay as highlighted in Figure 3a.

Distinct Disulfide Bond. The *A. oryzae* structure contains a unique disulfide bond between Cys63 and Cys76 that ties helix 2 to strand 2 of the central β -sheet (Figure 2a). This disulfide bond has not been previously reported for any cutinase or hydrolase structures.^{7,12–17} The other two disulfide bonds, Cys37–Cys115 connecting the loop between helix 1 and strand 1 with the loop between helix 4 and strand 3 and Cys177–Cys184 linking the loop following strand 5 to helix 9, are well-conserved in previously published cutinase structures, including that from *F. solani*.¹⁴ Sequence analysis suggests that this disulfide bond is unique for the cutinases from the *Aspergillus* family (sharing sequence identity of 50–77% with *A. oryzae*) and a few other filamentous fungi, such as *Neosartorya fischeri* (53% sequence identity) and *Emericella nidulans* (52% sequence identity) (Figure 2a). The cutinases from *F. solani* and *Glomerella cingulata* represent another group of filamentous fungi that do not have this special disulfide bond, although they share about 50% sequence identity with the *A. oryzae* enzyme.

Continuous Groove by the Active Site. Although the catalytic triad is sequentially conserved in both cutinases, they are topologically positioned differently. In the *A. oryzae* structure, His194 N δ 1 to Asp181 O δ 2 is 2.71 Å, and the Ser126 O γ to His194 N ϵ 2 is 2.63 Å (Figure 3b), which are within hydrogen bond distance. The corresponding distances in the *F. solani* cutinase are 2.84 Å for Asp175 O δ 2 to His188 N δ 1 and 2.98 Å from Ser120 O γ to His188 N ϵ 2, which is slightly larger than the hydrogen bond distance presented in the *A. oryzae* structure.¹⁶ This average distance of 2.98 Å was calculated on the basis of the presence of two possible positions of the Ser120 O γ in the native *F. solani* crystal structure: where the A form possesses a 73% occupancy and the B form a 27% occupancy (PDB ID:1CEX, Figure 3b). Moreover, the *A. oryzae* cutinase

(31) Benedict, C. V.; Cook, W. J.; Jarrett, P.; Cameron, J. A.; Huang, S. J.; Bell, J. P. *J. Appl. Polym. Sci.* **1983**, *28*, 327–334.(32) Nishida, H.; Tokiwa, Y. *J. Environ. Polym. Degrad.* **1993**, *1*, 227–233.(33) Murphy, C. A.; Cameron, J. A.; Huang, S. J.; Vinopal, R. T. *Appl. Environ. Microbiol.* **1996**, *62*, 456–460.

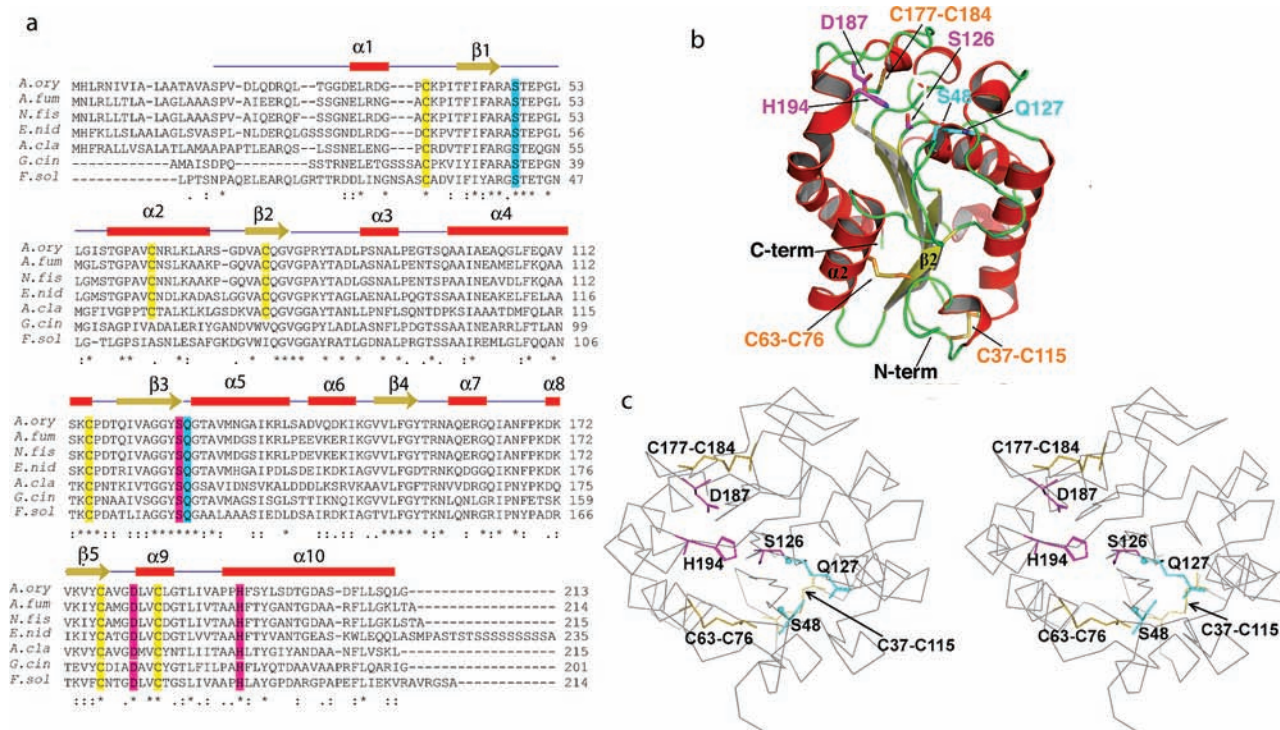


Figure 2. (a) Sequence alignment of *A. oryzae* cutinase with cutinases originating from representative filamentous fungi with sequence identity $\geq 50\%$. The α -helical regions are highlighted in red, β -strands in yellow, catalytic residues in magenta, oxyanion hole residues in cyan, and cysteines bearing disulfide bonds in yellow. Residues identical in all sequences in the alignment are labeled with “*”, residues with conserved substitutions are labeled with “:”, and semiconserved substitutions with “.”. The alignment was performed using NCBI BLAST (<http://blast.ncbi.nlm.nih.gov/>) and EBI ClustalW (<http://www.ebi.ac.uk/Tools/clustalw2/>). (b) Ribbon structure rendering of *A. oryzae* cutinase with the helices, strands, and catalytic residues labeled as in the alignment. The disulfide bonds between the cysteines are displayed in yellow. (c) Stereoview of *A. oryzae* cutinase with catalytic triad in magenta and oxyanion hole in cyan. Abbreviations: *Aspergillus oryzae*, *A.ory*; *Aspergillus fumigatus*, *A.fum*; *Aspergillus clavatus*, *A.cla*; *Emericella nidulans*, *E.nid*; *Neosartorya fischeri*, *N.fis*; *Glomerella cingulata*, *G.cin*; *Fusarium solani*, *F.sol*.

bears a longer and deeper groove by the active site relative to that of *F. solani* as demonstrated in Figure 3c. While the *A. oryzae* structure reveals a continuous groove that spans across the active site, the *F. solani* structure shows a narrow, shallower groove that abruptly stops. Gatekeepers of both cutinases with the esters of the active site demonstrate the presence of two gatekeeper residues (Leu87 and Val190) in *A. oryzae* and (Leu81 and Val184) in *F. solani* that play a role in substrate recognition (Figure 4). The two residues in *A. oryzae* residues are 9.87 Å ($C\beta$ to $C\beta$) apart, whereas the corresponding residues of the *F. solani* cutinase are separated by 8.74 Å. This results in the alkyl chain populations in *A. oryzae* laying across the wider groove region surrounding the active site, whereas for the *F. solani* model, there is a preponderance of alkyl chain structures that are oriented down the narrow tail of the groove.

Discussion

The molecular detail provided by the crystal structure elucidates the observed discrepancy in the activity and specificity of the two cutinases. The preference for the *A. oryzae* enzyme to hydrolyze longer chain substrates can be explained by the deep continuous groove extending across the active site, while that of *F. solani* favors short chain substrates due to the shallow and interrupted groove. This is further confirmed by our models demonstrating that the gatekeeper residues that line the groove within the *A. oryzae* are farther apart than the equivalent residues within the *F. solani* structure (Figure 4). In the *A. oryzae* structure, modeled with the hexanoate ester (Figure 4a), this additional space allows the carbon chains greater conformational freedom and easier access to a large region of the groove

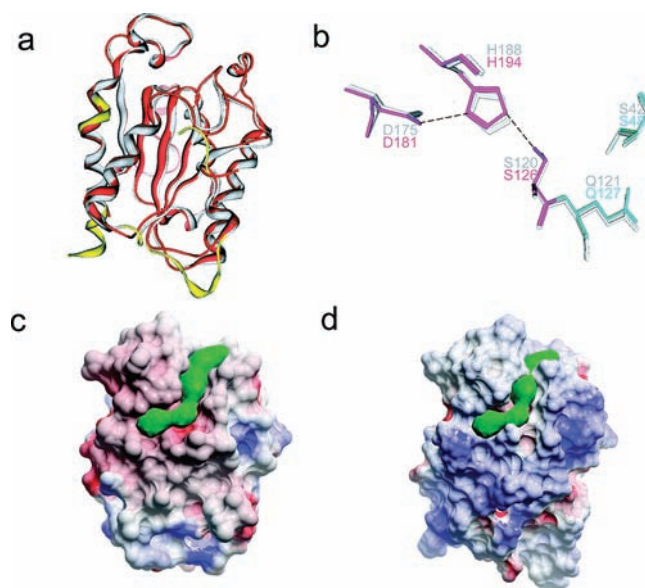


Figure 3. (a) Superposition of *A. oryzae* (red) and *F. solani* (gray) cutinases revealing nearly identical structural similarity. The nonoverlapping regions are highlighted in yellow. (b) Overlay of the *A. oryzae* cutinase (colored) residues of the catalytic triad and oxyanion hole with that of *F. solani* residues (gray). Residues are labeled accordingly. Electrostatic surface rendering of *A. oryzae* (c) and *F. solani* (d) cutinases as rendered by ICM software package.²⁸ The green solid density generated by the PocketFinder function of ICM illustrates the groove on the surface proximal to the active site.²⁸ Note that the green density cannot fit in the narrow groove on the *F. solani* cutinase.

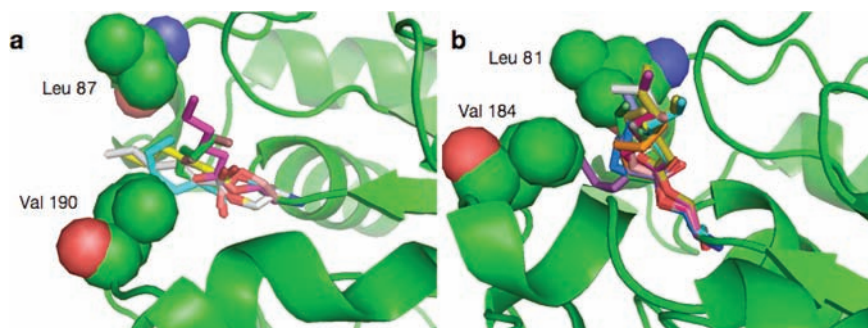


Figure 4. Predicted low energy conformations of serine hexanoate esters for (a) *A. oryzae* and (b) *F. solani* cutinases. Ester heavy atoms are shown as sticks for all conformations within 5 kcal mol⁻¹ of the lowest energy conformation after systematic screening of torsions and minimization. The gatekeeper residues, Leu87 and Val190 in *A. oryzae* and Leu81 and Val184 in *F. solani*, are shown as spheres.

surrounding the active site. However, in the *F. solani* structure (Figure 4b), the close distance between the two gatekeeper residues creates a barrier, constraining the alkyl chains to a narrower region of the groove pointing away from the active site. The presence of a wider, continuous groove by the opening of the active site in *A. oryzae* cutinase can also explain its ability to rapidly hydrolyze PCL relative to that of *F. solani* (Figures 3c and 4a).

Enhanced thermotolerance in comparison to that of *F. solani* is observed for *A. oryzae* cutinase by thermoactivity and thermodynamic stability experiments. This improved stability can be attributed to the presence of an additional disulfide bond as observed in the *A. oryzae* structure (Figure 2b). Specifically, the disulfide bond between Cys63 and Cys76 links a peripheral helix to the central β -sheet, providing extra stability. In general, covalent bonds stabilize proteins; specifically disulfide bonds connecting disparate and adjacent regions of a protein improves its thermostability.^{34–36}

Understanding how the cutinase structure plays an important role in function and stability not only provides insight into the reactivity of *A. oryzae* enzyme but also offers useful guidelines for the design of proteins in general. Much of the research on cutinases has thus far focused on that of *F. solani*. This is largely attributable to the existence of a crystal structure and extensive biochemical studies.^{16,18,37–40} Recently, the structure of *Glom-erella cingulata* cutinase has been determined, which suggests that the catalytic triad undergoes a significant conformational rearrangement during the catalytic cycle,⁴¹ providing insight into its reactivity. Although a large number of *other* cutinases have

been functionally investigated,^{18,37–40,42–45} none have been structurally characterized and linked to their reactivities.

Cutinases have demonstrated unique properties that can be exploited for degradation of various synthetic polymers and may in the near future find use in plastic recycling.⁴⁶ Critical features highlighted in this work include (i) engineering a continuous groove across the active site and (ii) including appropriate disulfide bonds as structural features that can be used in the redesign of other cutinases and related enzymes. From our studies, we have obtained useful guidelines for the redesign of proteins for environmentally compatible biocatalytic reactions on small molecules and polymer substrates useful for industry and academia.^{1–3} Further detailed characterization to elucidate structural and functional information are underway.

Acknowledgment. This work was supported in part by NYU-Poly Seed Fund (XPK, YG, RG and JKM), AFOSR DURIP (FA-9550-08-1-0266) (JKM), IUCRC (RG), NSF GK-12 Fellows grant 0741714 (PJB), NIH grant GM70841 (HL and XPK) and the HHMI Science education project at CCNY (YG, ZL and GA). We thank Jeremy Minshull and Jonathan Ness from DNA 2.0 for their assistance with DNA and protein expression and purification optimization.

Supporting Information Available: The coordinates of the *A. oryzae* cutinase structure are available in the protein data bank with the ID 3GBS. SDS PAGE, CD, DSC and modeling characterization as well as kinetics is available free of charge via the Internet at <http://pubs.acs.org>.

JA9046697

(34) Pace, C. N. *J. Mol. Biol.* **1992**, *226*, 29–35.

(35) Green, S. M.; Meeke, A. K.; Shortle, D. *Biochemistry* **1992**, *31*, 5717–5728.

(36) Doig, A. J.; Williams, D. H. *J. Mol. Biol.* **1991**, *217*, 389–398.

(37) Abergel, C.; Martinez, C.; Fontecillacamps, J.; Cambillau, C.; Degeus, P.; Lauwereys, M. *J. Mol. Biol.* **1990**, *215*, 215–216.

(38) Longhi, S.; Manesse, M.; Verheij, H. M.; DeHaas, G. H.; Egmond, M.; KnoopsMouthuy, E.; Cambillau, C. *Protein Sci.* **1997**, *6*, 275–286.

(39) Longhi, S.; Nicolas, A.; Creveld, L.; Egmond, M.; Verrips, C. T.; deVlieg, J.; Martinez, C.; Cambillau, C. *Proteins: Struct. Funct. Genet.* **1996**, *26*, 442–458.

(40) Ettinger, W. F.; Thukral, S. K.; Kolattukudy, P. E. *Biochemistry* **1987**, *26*, 7883–7892.

(41) Nyon, M. P.; Rice, D. W.; Berrisford, J. M.; Hounslow, A. M.; Moir, A. J. G.; Huang, H. Z.; Nathan, S.; Mahadi, N. M.; Abu Bakar, F. D.; Craven, C. J. *J. Mol. Biol.* **2009**, *385*, 226–235.

(42) Nielsen, A. D.; Arleth, L.; Westh, P. *Biochim. Biophys. Acta* **2005**, *1752*, 124–132.

(43) Figueroa, Y.; Hinks, D.; Montero, G. *Biotechnol. Prog.* **2006**, *22*, 1209–1214.

(44) Genencor, Cutinase for use in detergent composition produced by culturing *Pseudomonas putida*, U.S. Patent 89-02922, 1988.

(45) Yoon, M. Y.; Kellis, J.; Poulouse, A. J. *AATCC Rev.* **2002**, *2*, 33–36.

(46) Seo, H. S.; Um, H. J.; Min, J.; Rhee, S. K.; Cho, T. J.; Kim, Y. H.; Lee, J. *FEMS Yeast Res.* **2007**, *7*, 1035–1045.